Geomorphology 265 (2016) 107–116

Contents lists available at ScienceDirect

Geomorphology

journal homepage: www.elsevier.com/locate/geomorph

Monitoring channel head erosion processes in response to an artificially induced abrupt base level change using time-lapse photography

M.H. Nichols *, M. Nearing, M. Hernandez, V.O. Polyakov

Southwest Watershed Research Center, USDA-ARS, 2000 E. Allen Rd., Tucson, AZ 85719, USA

ARTICLE INFO

Article history:
Received 31 July 2015
Received in revised form 27 January 2016
Accepted 1 May 2016
Available online 7 May 2016

Keywords:
Gully erosion
Piping
Subsurface erosion
Time-lapse photography

ABSTRACT

Gullies that terminate at a vertical-wall are ubiquitous throughout arid and semiarid regions. Multi-year assessments of gully evolution and headcut advance are typically accomplished using traditional ground surveys and aerial photographs, with much recent research focused on integrating data collected at very high spatial resolutions using new techniques such as aerial surveys with blimps or kites and ground surveys with LiDar scanners. However, knowledge of specific processes that drive headcut advance is limited due to inadequate observation and documentation of flash floods and subsequent erosion that can occur at temporal resolutions not captured through repeat surveys. This paper presents a method for using very-high temporal resolution ground-based time-lapse photography to capture short-duration flash floods and gully head evolution in response. In 2004, a base level controlling concrete weir was removed from the outlet of a 1.29 ha semiarid headwater drainage on the Walnut Gulch Experimental Watershed in southeastern Arizona, USA. During the ten year period from 2004 to 2014 the headcut migrated upchannel a total of 14.5 m reducing the contributing area at the headwall by 9.5%. Beginning in July 2012, time-lapse photography was employed to observe event scale channel evolution dynamics. The most frequent erosion processes observed during three seasons of time-lapse photography were plunge pool erosion and mass wasting through sidewall or channel headwall slumping that occurred during summer months. Geomorphic change during the ten year period was dominated by a single piping event in August 2014 that advanced the channel head 7.4 m (51% of the overall advance) and removed 11.3 m^3 of sediment. High temporal resolution time-lapse photography was critical for identifying subsurface erosion processes, in the absence of time-lapse images piping would not have been identified as an erosion mechanism responsible for advancing the gully headwall at this site.

Published by Elsevier B.V.

1. Introduction

Incised, or gullied, channels that terminate at a vertical-wall are common features in semiarid watersheds. The geomorphic evolution of gullied channels is often dominated by migration of the headwall, and quantifying multi-year (Montgomery, 1999; DeLong et al., 2014) and multidecadal (Rieke-Zapp and Nichols, 2011; Frankl et al., 2012; Rengers and Tucker, 2014) rates of headcut advance has been the focus of many studies. Knowledge of long-term rates of headcut retreat have been useful for interpreting the effects of land use change (Trimble, 1999; Frankl et al., 2012) and in providing a basis for fundamental comparison among varying landscapes. However, long-term rates provide no information on erosion process dynamics and interactions with hydrologic drivers that are fundamental to furthering our understanding of semiarid geomorphic systems.

Gullies are an important sediment source in drylands, contributing between 50% and 80% of overall sediment production (Poesen et al., 2003). In the southwestern US, headcutting was shown to produce a significant portion of the total sediment load from a 200 ha watershed monitored for 20 years on the USDA-ARS Walnut Gulch Experimental Watershed (WGEW) (Osborn and Simanton, 1986). The sediment contribution from gully banks and headcuts in a discontinuous ephemeral gully system within which a sand bottom channel extends through a broad swale terminating at a near vertical headwall was estimated to be about 25% of the suspended sediment load sampled downstream from the headcut (Osborn and Simanton, 1986). In a more recent study of this gully system, retreat rate was found to be a function of drainage area and 30 min rainfall intensities above 25 mm h^{-1} (Rieke-Zapp and Nichols, 2011). At the spatial scale of approximately 10 ha within the WGEW, small gullied watersheds can produce up to three times the total sediment load as similar-sized nongullied watersheds (Osborn et al., 1976). A sediment budget developed for a 43.7 ha watershed within WGEW revealed that hillslope interfluve areas were the dominant source of sediment (Nichols et al., 2013); however, the authors acknowledged the lack of measurements to explicitly quantify channel process including bank sloughing and erosion. These studies point to the need for additional research to understand the processes involved in sediment production from channels.

* Corresponding author.
E-mail address: mary.nichols@ars.usda.gov (M.H. Nichols).

http://dx.doi.org/10.1016/j.geomorph.2016.05.001
0169-555X/Published by Elsevier B.V.

The mechanisms of channel head erosion are many and varied (Dietrich and Dunne, 1993). Plunge pool erosion and impinging jet scour followed by collapse play an important role in headcut migration (Alonso et al., 2002; Flores-Cervantes et al., 2006). Subsurface flow and seepage erosion play an important role in gully development and streambank failure (Dunne, 1990; Bryan and Jones, 1997; Faulkner, 2006), and piping has been identified as a factor in channel head development (Leopold and Miller, 1956; Parker, 1963; Fox and Wilson, 2010; Wilson, 2011). Other mechanisms of erosion include saturation slumping and mass failure of channel banks. When the shear strength of the bank is exceeded, rapid rotational slip (Alonso and Combs, 1990) can contribute large amounts of sediment directly to the channel. All of these erosion mechanisms are affected by topography, parent material, and soil characteristics. Although the regionally important mechanisms of channel erosion listed above have been the subject of a large body of research, these processes have not received much research attention on the WGEW.

Field data and observations describing event scale erosion dynamics in semiarid systems are rare; in large part because collecting data associated with infrequent and unpredictable runoff events is logistically difficult. Recent advances in sensor and datalogging technologies have made it possible to conduct field studies of event scale channel erosion dynamics (DeLong et al., 2014; Rengers and Tucker, 2014). As pointed out by Poesen et al. (2011) the significant interactions between gully erosion and hydrological processes need to be better understood for improving our predictions of hydrological response and land degradation rates under different environmental conditions. Field research is needed to determine modes of gully erosion and quantify relationships among precipitation, runoff, and geomorphic change.

Intensively instrumented low-order watersheds within the WGEW offer the opportunity to expand previous studies to quantify channel evolution (Osborn and Simanton, 1986, 1989) and watershed sediment yields (Nichols, 2006; Nearing et al., 2007) to include gully erosion process dynamics. Although understanding semiarid erosion processes has been a primary objective of research on the WGEW since its establishment in 1953, field research has focused on surface rill and interrill erosion process, primarily at the plot scale. Recent research based on tracer studies has expanded the scale of surface erosion to hillslopes and small watersheds (Nearing et al., 2005; Polyakov et al., 2009). Despite the wealth of erosion research on the WGEW, gully erosion processes have received limited attention. The objective of this study is to identify the dominant channel erosion processes and quantify short-term headcut and channel evolution in a low-order watershed within the WGEW.

2. Study site

This study was conducted from 2004 to 2014 in the Lucky Hills subwatersheds within the 150 km^2 WGEW in southeastern Arizona (Fig. 1). From 2004 through 2014, the linear rate of headcut advance was measured, and beginning in 2012, detailed storm event-based observations were made during three runoff seasons.

2.1. Climate, vegetation, and soils

The climate of southeastern Arizona is semiarid and mean annual precipitation measured on the WGEW for the 50 year period from 1956 to 2005 was approximately 312 mm (Goodrich et al., 2008). The precipitation distribution is bimodal with approximately 2/3 generated during the summer monsoon months (July to September) resulting from intense, convective thunderstorms, and the remaining 1/3 originating from less intense frontal storms during winter months. Almost all runoff on the WGEW is generated during summer months with occasional fall and winter runoff, and the main Walnut Gulch channel is dry 99% of the time. Channel runoff occurs in discrete, short duration flash floods lasting from minutes to hours with hydrographs characterized by a rapidly rising limb followed by a tapering recession.

Vegetation at Lucky Hills is dominated by shrubs including whitethorn Acacia [*Acacia constricta* Benth.], Tarbush [*Flourensia cernua* DC], and Creosote [*Larrea divaricata* Cav.] (King et al., 2008). A sparse understory of grasses and forbs is also found (Weltz et al., 1994). Locally, vegetation at the headcut site responds dynamically to monsoon precipitation and grass cover increases through the summer months with an associated reduction in bare soil. During the summer season canopy cover is approximately 25% with only minor amounts of litter on the ground. Although historically grazed, the Lucky Hills complex has been fenced to exclude grazing since 1963.

Soils on the watershed hillslopes are primarily gravelly sandy loams with approximately 39% gravel, 32% sand, 16% silt, and 13% clay and a high fraction (46%) of fragmented rocks (USDA, 2003). The parent material is mixed calcareous fan alluvium and the surface is generally rock covered. Soils are classified as Luckyhills-McNeal (very deep, well drained nearly level to strongly sloping, gravelly moderately coarse and moderately fine textured soils on fan terraces). Classifications for the Lucky Hills soils are coarse-loamy, mixed, thermic Ustic Haplocalcids and the McNeal soils are fine-loamy, mixed, thermic Ustic Calciargids. The gravelly loam layer covers coarse textured calcareous soils that show little soil profile development and an A horizon from 0 to 5 cm deep (USDA, 2003).

2.2. Geomorphic setting

The WGEW is located on an alluvial fan in the basin and range physiographic province in southeastern Arizona surrounding the town of Tombstone. The headwaters are located in the Dragoon Mountains to the east, and the generally westward draining watershed is tributary to the San Pedro River. The San Pedro River entrenched between 1890 and 1908 (Hereford, 1993) and currently, the channel network on the lower end of the WGEW is evolving in response to the resultant energy gradient (Osterkamp, 2008).

A distinct geologic feature of the WGEW is a fault that cuts through the watershed from south to north (Fig. 1). The fault line defines two landscape surfaces characterized by distinct erosional processes that have yielded geomorphic surfaces of varying ages and evolutionary stage (Osterkamp, 2008). The Whetstone Pediment lies to the east of the fault. The upper part of the Whetstone Pediment is characterized by a pattern of swales and headcuts typical of a discontinuous ephemeral stream pattern described by Bull (1997). Headcut migration rates in this area over a 70 year period range from 0.35 to 1.5 m year^{-1} (Rieke-Zapp and Nichols, 2011).

The lower, westerly, part of the Whetstone Pediment, called the Dissected Whetstone Pediment, and the Tombstone surface to the west of the fault on the lower end of the watershed, are characterized by a well-developed, incising channel network. Most of the sediment delivered from the WGEW is generated from the Dissected Whetstone Pediment and the Tombstone Surface (Graf, 1983).

In addition to topographic energy differentials, lithology exerts strong control on erosional processes. Within WGEW, the underlying geology imposes spatial control on channel network evolution. For example, in general, channels on the lower end of the watershed incise until they reach the underlying Emerald Gulch conglomerate which provides a base level that is resistant to erosion. Subsequent channel adjustment occurs as headward migration.

The study site and monitored headcut are located in the intensively monitored Lucky Hills (LH) subwatershed complex (Fig. 2) which is located on the Dissected Whetstone Pediment (Fig. 1). Between the measuring stations at LH101 and LH103, the watershed is drained by a well-defined channel network. The main stem and tributaries are continuous, single thread and incised with near vertical walls in some sections. The main channel bed consists of alluvial sediment ranging in size from sands to cobbles.

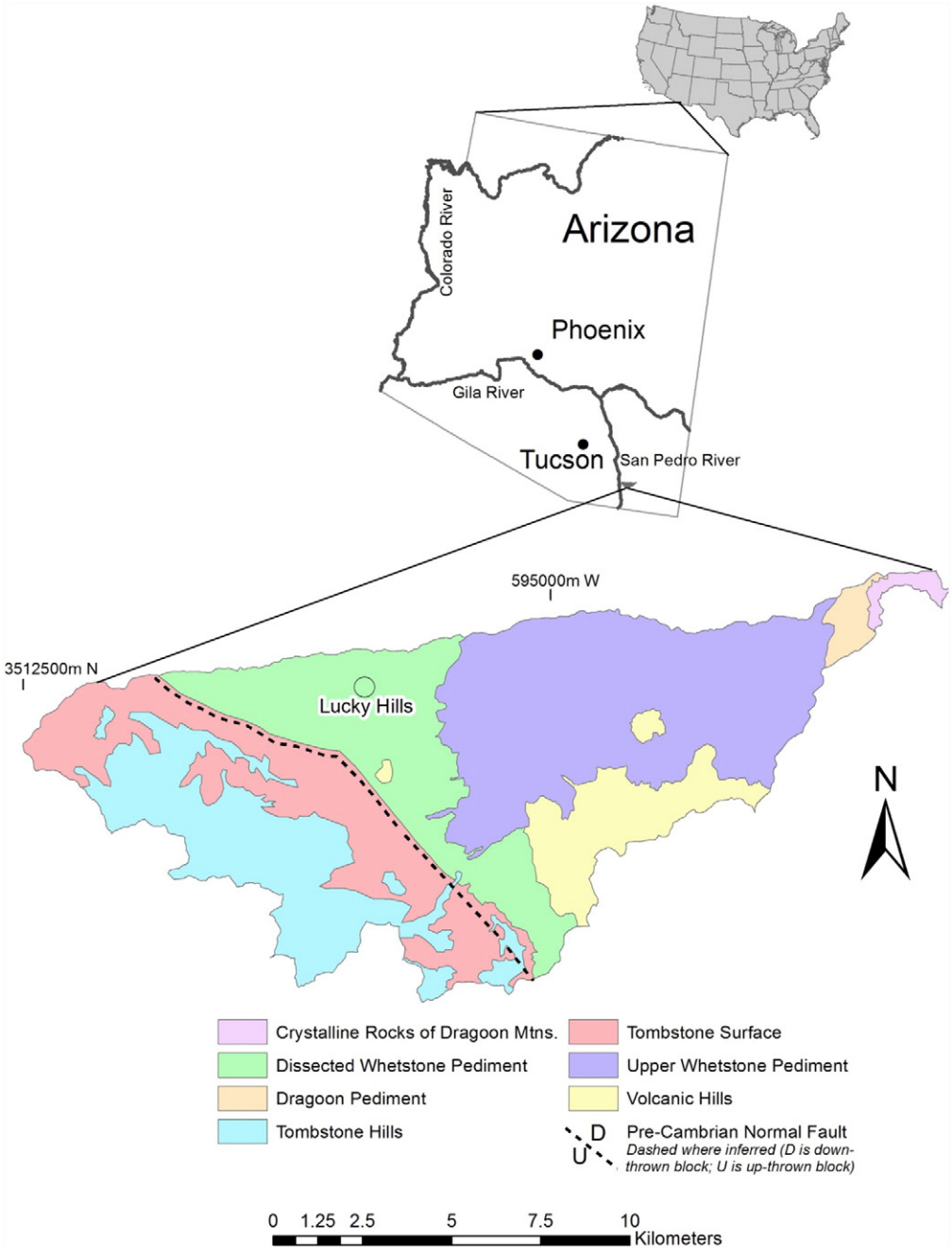

Fig. 1. Walnut Gulch Experimental Watershed and Lucky Hills headcut study site location map showing major geomorphic features including erosional surfaces and pediments, and a high-angle normal fault (after Osterkamp, 2008).

Prior to 2004, the upper end of the main LH103 channel terminated at measurement station LH101, which consisted of a concrete V-notch weir (Stone et al., 2008) located at the outlet of the upper 1.29 ha headwaters. Accurate measurement with the weir was complicated by loss of hydraulic control through the V-notch as sediment was deposited in the stilling basin leading to the weir and although the structure remained onsite, measurement was discontinued in 1986. The hydraulic structure at LH101 provided an artificial control on base level lowering and landscape evolution. A distinct layer of deposited sediment approximately 20 cm deep at its maximum overlying the pre-instrumentation gravel covered landscape is easily identified in the field. Within the 1.29 ha watershed overland flow erosion and drainage patterns are highly dynamic as observed by the authors through measurement of erosion pins. The V-notch weir was removed in 2004 with the objective of studying the evolution of the channel network and the adjacent landscape in response to the abrupt base level change. Removal was expected to rejuvenate the headcut and tributaries in response to the elevation offset from the main channel bottom to the landscape surface. Currently, the incising main channel terminating at a 1.0 m high headwall is the dominant geomorphic feature of the landscape.

It is important to note that surface soil disturbance associated with weir removal created an altered landscape that extended approximately 3 m upstream of the weir site. The disturbance resulted in local removal of sediment deposited in response to the weir and a local region of bare soil with very few small creosote bushes. By 2012, when the time-lapse camera system to observe event scale erosion processes was installed, the headcut had advanced through most of the altered surface.

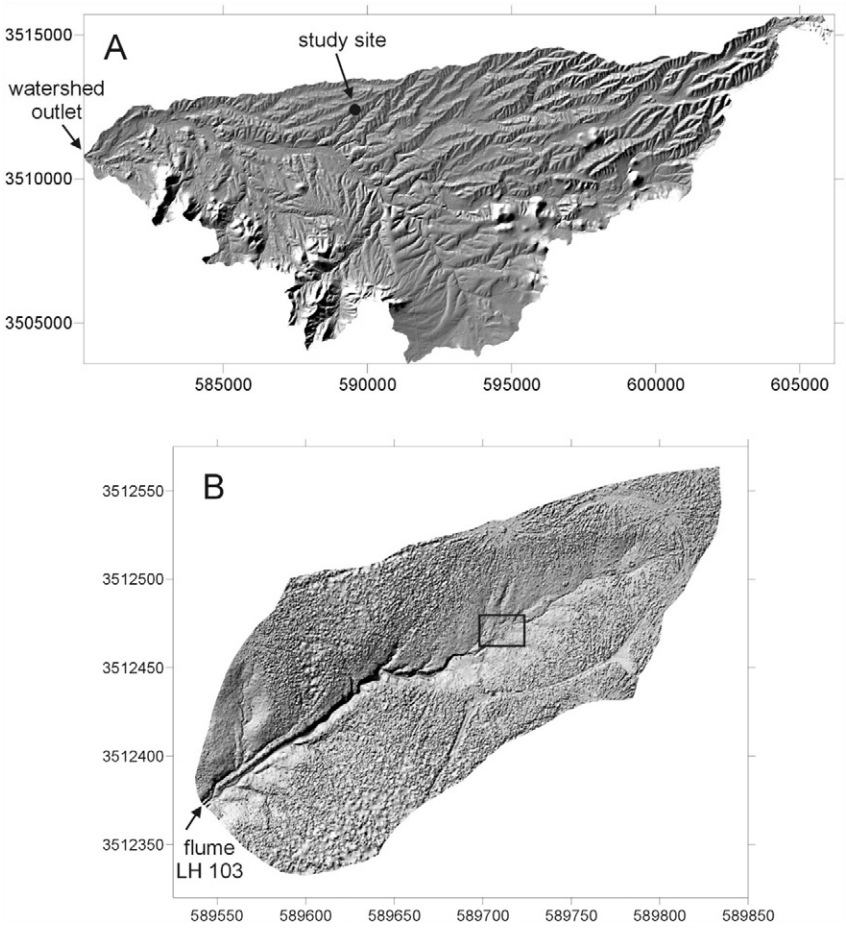

Fig. 2. Shaded-relief image of the Walnut Gulch Experimental Watershed (A) illustrating drainage patterns and detailed image of the Lucky Hills study site (B) with a rectangle bounding the headcut measurement area. Axes are labeled with UTM coordinates. North is up.

3. Methods

3.1. Topographic measurement (2004–2014)

Conventional topographic surveys were conducted annually with a total station in 2005 through 2008 to delineate the planform extent of the channel head. Equipment and personnel limitations precluded surveying from 2009 to 2012. Ground-based LiDar was used to scan the site in July 2013 (Leica C10 Scan Station) and again in October 2014 (Riegl VZ 400). Horizontal and vertical control for the conventional and LiDar surveys was provided by permanent benchmarks that were used to register sequential surveys. Logistical constraints precluded surveying after every storm event. Volume change between scan dates was accomplished using digital elevation model comparison and 3-D change detection.

3.2. Hydrologic data and modeling (2012–2014)

The study site is instrumented to measure precipitation, runoff, and soil moisture. Precipitation is measured with a digital recording rain gauge at a temporal resolution of 1 min (Keefer et al., 2008). LH101 is nested within LH103 (Fig. 2). Runoff was measured at LH103, which is located 160 m below LH101 at the outlet of 3.68 ha (9.1 acres), with a Santa Rita supercritical flume (Smith et al., 1982; Fig. 2). The KINEROS2 rainfall-runoff simulation model (Smith et al., 1995; Goodrich et al., 2012) was calibrated using measured precipitation data and runoff measured at LH103 (Fig. 3). The model is a physically based approach to modeling overland flow as a kinematic wave. The calibrated model was used to compute event runoff volume and peak discharge rates at the headcut site based on measured rainfall. The proximity of LH103 and LH101, with LH101 nested within the LH103 watershed, and the very high correlation between observed and simulated runoff ($R^2 = 0.99$) and peak runoff rate ($R^2 = 0.99$) at LH103, provide a high degree of confidence in simulated values for LH101. Runoff durations were determined from time-lapse photography, which also provided verification of model results.

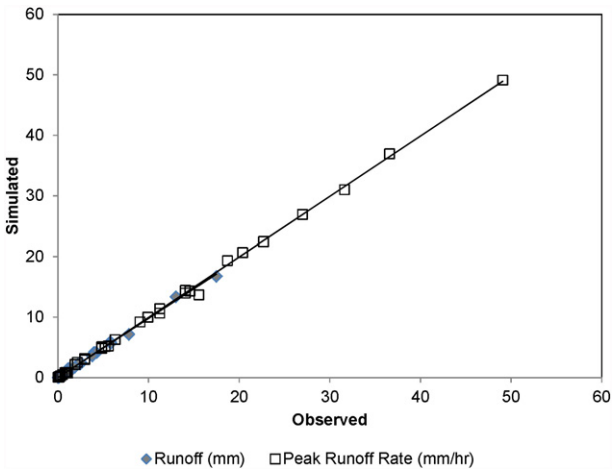

Fig. 3. Observed runoff volume and peak runoff rates measured at LH103 in comparison with KINEROS2 simulated values.

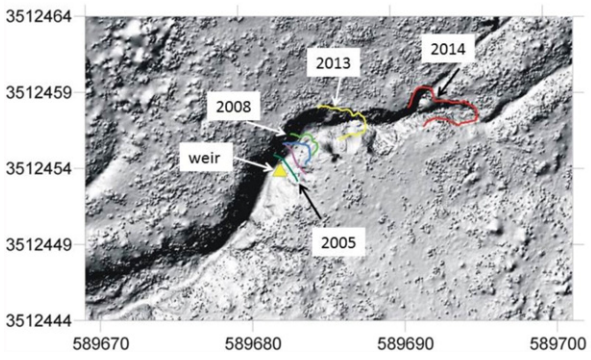

Fig. 4. Headwall locations from 2005 through 2014 against a 2014 image of the headcut study site.

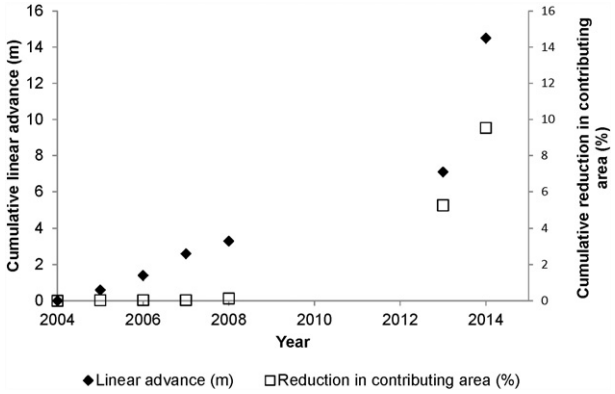

Fig. 5. Cumulative linear rate of headcut advance and resultant cumulative reduction in runoff contributing area from 2004 through 2014.

Volumetric soil water content was measured using time domain reflectometry probes at five different profile locations across the watershed (Keefer et al., 2008). Four profiles were within approximately 100 m of the headcut site with the fifth at approximately 200 m. Data collected at depths of 5 cm are reported as a daily average of all five profiles.

3.3. Time-lapse photography (2012–2014)

High temporal resolution time-lapse photography was used to observe hydrologic drivers and erosion response at the headcut. A Canon A800 off the shelf point and shoot digital camera was mounted inside a weatherproof Pelican case. The camera power supply was modified to run from a 12 V car battery that was charged with a 25 W solar panel. Ten MP images were collected from 12:00 noon through 7:00 pm every 30 s during three July–September monsoon runoff seasons. Camera-based observation began in July 2012 and continued through September 2012. The camera did not operate during the 2012–2013 winter months, but was redeployed in July 2013 and operated through September 2014. Thus we were able to capture images during the months between the 2013 and 2014 monsoon runoff seasons, although the time step was increased to every 30 min. The field of view included the headcut and immediate surroundings.

Control over image capture was accomplished programmatically. CHDK (http://chdk.wikia.com/wiki/CHDK), a free firmware enhancement that allows for programmatic camera control, was used to run a script that specified the start and stop time, shot interval, zoom, and focal distance. CHDK was installed on the camera's memory card along with a script to accomplish the time-lapse imaging. Individual still images were stitched to created videos using Microsoft Movie Maker and Adobe Premiere Elements.

Runoff observed through the photo sequences provided evidence and validation of modeled runoff, and event durations were quantified from image timestamps. Prior to the acquisition of a ground based LiDar scanner, no attempt was made to quantify volumes associated with observed geomorphic change. Event based topographic change was observed through time-lapse photograph sequences, although not explicitly quantified. Observed erosion processes were categorized from 0 to 4 according to the following descriptions: 0 – no change observed, 1 – dry ravel and minor sediment grain movement, 2 – scour at channel headwall or channel banks, 3 – plunge pool erosion and channel head or bank slumping, and 4 – geomorphically significant change. Although these categories impose somewhat arbitrary qualitative bounds on complex processes that may mutually contribute to overall change, they provide a basis for relating geomorphic response to hydrologic drivers and allow us to quantify the range of precipitation and runoff conditions associated with each categorized erosion process.

Table 1
Summary of linear headcut advance and resultant change in runoff contributing area.

Time period	Linear advance (m)	Change in contributing area %
2004–2005	0.6	0.3
2005–2006	0.8	<0.01
2006–2007	1.2	<0.01
2007–2008	0.7	0.09
2008–2013	3.8	5.14
2013–2014	7.4	4.27
2004–2014	14.5	9.5

4. Results

4.1. Linear retreat and watershed area change (2004–2014)

At the end of the 2014 monsoon season, the headwall was 14.5 m from the prior weir location at LH101 (Fig. 4), and the contributing area at the channel headwall was reduced by 9.5%. The average retreat rate over the 10 year period was 1.45 m year^{-1} (Table 1). Cumulative retreat rates and associated reduction in cumulative runoff contributing area (Fig. 5) increased sharply in 2014, and detailed storm event measurements and erosion observed through time-lapse photography from 2012 to 2014 presented in the following sections are critical for interpreting average annual retreat rate.

4.2. Precipitation, runoff, soil moisture (2012–2014)

All of the runoff at the headcut site was generated during summer months; there were no runoff events during non-monsoon season months. Although the total number of precipitation events did not vary considerably across the summer seasons, there were three times more runoff events in 2014 (18 events) than in 2012 (six events) (Table 2). Monsoon season precipitation/runoff ratio varied from 9 (2013) to 12 (2012).

Total runoff producing precipitation in 2014 (282.2 mm) was more than twice that in 2012 (112.6 mm) (Table 2). In addition, 52% (146.5 mm) of the runoff producing precipitation in 2014 was generated during three days. A wide range in precipitation totals is not unexpected on the WGEW where interannual variability of both seasonal and annual precipitation totals have been shown to exhibit high variability (Nichols et al., 1993; Goodrich et al., 2008).

Characteristics of individual runoff events at the headcut site are presented in Table 3. Modeled event runoff ranged from 0.005 to 15.8 mm, with monsoon season totals ranging from 15.4 to 32.7 mm. Runoff event durations observed through time-lapse imagery ranged from 14 to 51 min. Typically, runoff was generated in response to high intensity convective thunderstorms. An exception to this pattern occurred in September 2014. Precipitation patterns in September 2014

Table 2
Summary of precipitation and modeled runoff at LH101 from 2012 to 2014.

		Precipitation (mm)	Runoff producing precipitation (mm)	Runoff volume (mm)	Number of precipitation events	Number of runoff events
2012	Monsoon season	191	113	15	31	6
	Winter	68		0	20	0
	Total	240				
2013	Monsoon season	228	174	25	29	10
	Winter	47		0	11	0
	Total	287				
2014	Monsoon season	344	282	33	32	18
	Winter	68		0		0
	Total	412				

were dominated by two Pacific hurricanes that yielded distinct runoff responses. A decaying hurricane event on September 8 delivered 60.5 mm of precipitation over 261 min and yielded 15.8 mm of runoff during a 50 min flow (46% of the 2014 total runoff). The storms of September 17 and 18 were remnant of Hurricane Odile and were characterized by persistent, long duration, relatively low intensity precipitation. Although the total precipitation during the September 17 and 18 storms was 86 mm (30% of the monsoon season total), the total runoff volume was small (5.64 mm or 16% of the 2014 total runoff).

Relationships among precipitation, runoff, and soil moisture are shown in Fig. 6. Volumetric soil moisture response in the top 5 cm of soil exhibited a rapid increase in response to storms followed by drying between storms (Fig. 6). Because of very high evaporation rates and shallow infiltration depths, soil moisture fluxes within the Lucky Hills area are most pronounced in the upper 5 cm of soil, and at 30 cm of depth, measured soil moisture is relatively constant. As a general indicator of the relation between erosion processes and soil moisture fluxes, erosion codes assigned to individual precipitation events were plotted against the difference in volumetric water content on the day of precipitation and the day after. Fig. 7 shows the wide range in soil moisture flux conditions that yield generally similar erosion responses. The occurrence of dry ravel and minor grain movement as well as saturation slumping and mass wasting all occur under both drying and wetting conditions. Although antecedent moisture in the upper 5 cm soil layer is a relatively unimportant controlling factor in runoff generation on the Lucky Hills watersheds (Goodrich et al., 1994; Zhang et al., 2011), wetting of the banks was observed to be followed by collapse and slumping (Fig. 8) and thus soil moisture appears to be an important controlling factor in channel erosion dynamics. More detailed field measurements are needed to quantify the processes and drivers. Because

Table 3
Characteristics of precipitation and runoff for individual events at Lucky Hills 101 during the 2012, 2013, and 2014 monsoon seasons.

Date (mm/dd/yyyy)	Precipitation				Runoff			
	Start time	Duration (min)	Max I30 (mm h^{-1})	Volume (mm)	Volume (mm)	Peak rate (mm h^{-1})	Duration (min)	Night flow
7/3/2012	20:23	155	51	33	4	10		x
7/4/2012	14:56	128	20	15	2	8	30	
8/7/2012	20:58	20	21	10	1	7		x
9/3/2012	16:59	209	27	30	4	13		
9/5/2012	2:19	113	11	6	0	0		
9/6/2012	16:29	28	38	19	5	26		
Total				113	15			
7/7/2013	15:17	71	33	24	1	3		
7/9/2013	21:25	56	20	11	1	5		x
7/11/2013	23:27	110	20	13	2	9		x
7/19/2013	12:36	41	26	14	1	4	36	
7/25/2013	14:32	61	15	8	0	1	20	
8/2/2013	12:31	86	37	24	5	16	51	
8/12/2013	15:51	67	18	13	0	2	37	
8/29/2013	11:11	43	12	7	0	1		
8/29/2013	13:52	11	17	9	2	9	30	
9/12/2013	18:54	188	56	51	13	40		x
Total				174	25			
7/11/2014	20:00	89	13	8	0	0		x
7/12/2014	19:39	92	16	11	0	3		x
7/14/2014	20:11	107	3	3	0	0		x
7/15/2014	13:15	24	10	5	0	1	14	
7/25/2014	16:32	35	17	9	0	1	17	
8/1/2014	21:14	93	44	26	7	19		x
8/9/2014	17:04	448	10	14	0	0		
8/12/2014	19:55	153	12	9	0	4		x
8/13/2014	18:04	130	10	8	0	0	20	
8/15/2014	16:19	87	29	18	4	16	48	
8/16/2014	18:54	111	18	15	1	2		x
8/17/2014	18:49	165	15	10	1	3		x
9/8/2014	12:14	261	60	60	16	34	50	
9/16/2014	1:39	221	3	6	0	0		x
9/17/2014	0:50	177	14	15	1	7		x
9/17/2014	11:41	81	10	6	0	2	21	
9/17/2014	15:27	563	17	39	3	10		x
9/18/2014	1:52	344	11	20	1	2		x
Total				282	34			

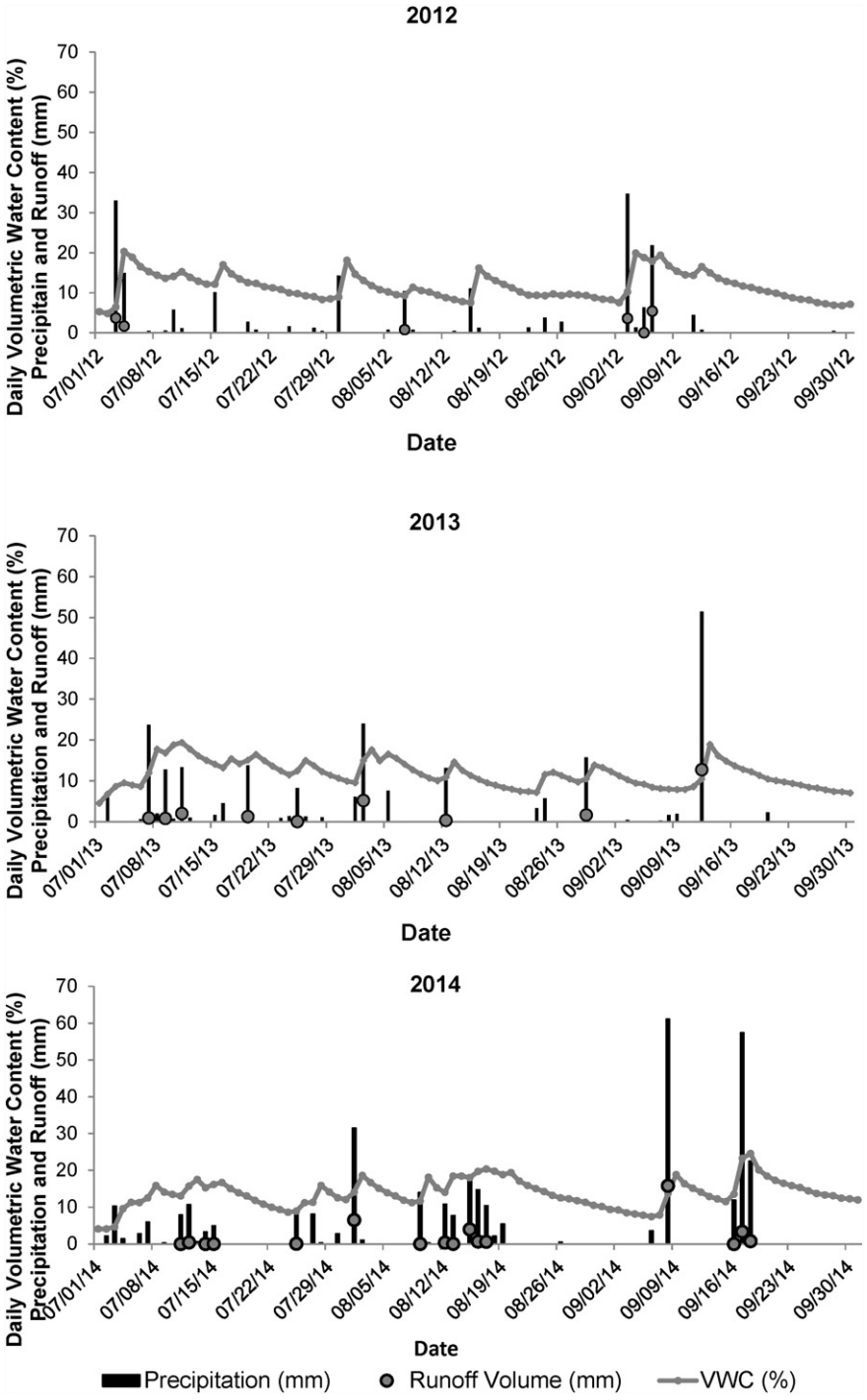

Fig. 6. Continuous daily volumetric water content (%) with precipitation and runoff plotted for the 2012, 2013, and 2014 monsoon seasons. Dates are formatted as mm/dd/yy.

infiltration and soil moisture distribution are highly spatially heterogeneous on the WGEW (Stillman et al., 2014), determining threshold soil moisture conditions for channel bank erosion will require installation of sensors in very close proximity or adjacent to the channel.

4.3. Observations of erosion during individual events (2012–2014)

By 2012 the headwall had moved approximately 3 m through the deposition zone that was induced by the presence of the base level controlling weir, and subsequent erosion was observed through time-lapse photography. Sediment had eroded from underneath the headwall leaving an overhanging headwall face and south channel bank. Observations of runoff and erosion dynamics were limited to daylight hours when the camera was capturing images. A total of 18 runoff events were photographed offering the opportunity to observe hydrologic response, the mechanisms of erosion, and channel erosion dynamics. Three daytime flows in 2012 and one in 2013 were not photographed due to camera problems. Overall, 16 of the 34 flows occurred at night and interpretation of erosion dynamics for these events was limited to before and after event imagery.

During the 2012 monsoon season, only one of the six runoff events was fully photographed (images every 30 s for the duration of the event). During the 30-min flow runoff overfall was observed at the headwall and also along the channel banks. The five additional events

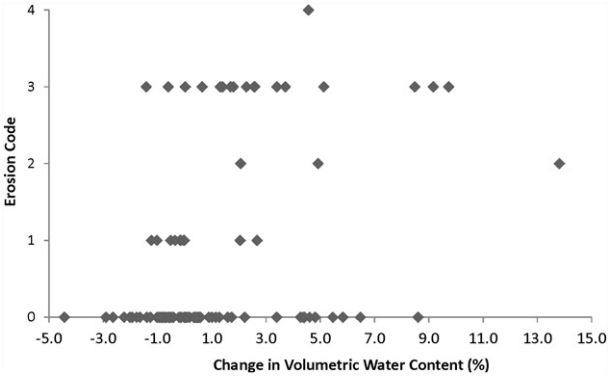

Fig. 7. Categorized erosion (0 – no change observed, 1 – dry ravel and minor sediment grain movement, 2 – scour at channel headwall or channel banks, 3 – plunge pool erosion and channel head or bank slumping, and 4 – geomorphically significant change) with respect to soil moisture fluxes. The change in volumetric water content (*VWC*) was calculated as the difference between *VWC* measured on the day of a precipitation event and *VWC* measured on the following day. Negative changes in *VWC* indicated drying, and positive changes in *VWC* indicate wetting.

were evaluated through before and after photographs. The primary erosion mechanism was slumping at the headwall (Fig. 8); however, observations of slumping during the July 4, 2012 event revealed that the slumping was not coincident with runoff peak, but occurred during flow secession.

During the 2013 monsoon season, five runoff events were fully photographed. During three of the events the dominant erosion mechanism was observed to be plunge pool erosion, and no bank slumping was observed during these flow. On August 12, 2013 headwall slumping was observed. Between monsoon seasons during the 2013–2014 winter months, dry ravel and minor sediment grain movement were observed both in response to precipitation and in the absence of precipitation.

During the 2014 monsoon season runoff and erosion dynamics were observed during six of 18 runoff events. Undercutting at the headwall

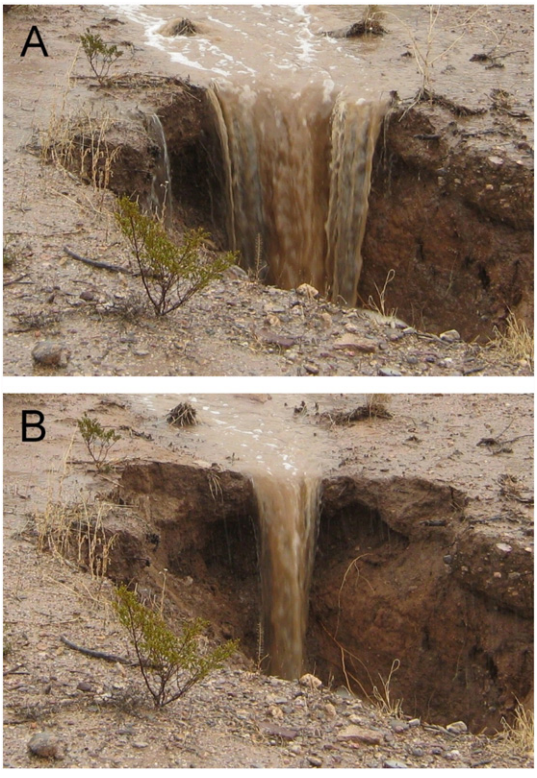

Fig. 8. Slumping at the headwall. (A) Captured during a 30 min runoff event on July 4, 2012 at 4:49 pm. (B) Captured at 4:54 pm.

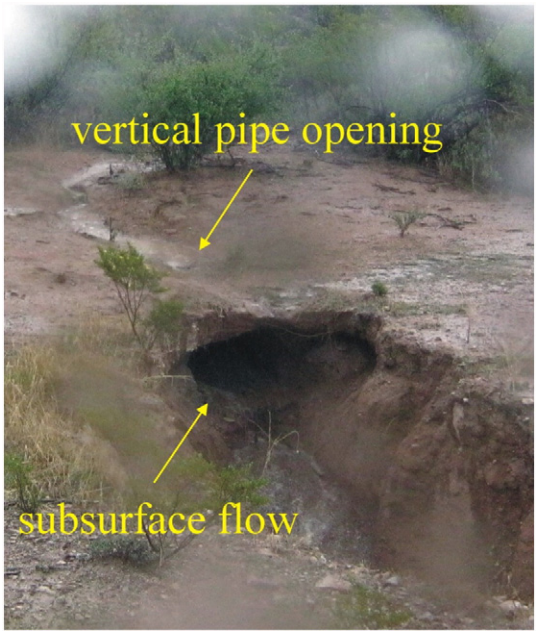

Fig. 9. Image of July 25, 2014 surface runoff that was diverted into a vertical pipe resulting in subsurface erosion. A time-lapse video of this erosion event can be seen by clicking on the photo.

was observed following the event of July 12, 2014. On July 15, 2014 overfall at the headwall was limited to a slight trickle, but ponding was observed in the channel above the headwall during flow recession. Field inspection revealed a 20 cm diameter vertical pipe opening in the unincised approach channel that connected to a subsurface horizontal trench. Runoff on July 25, 2014 was fully captured through the pipe (Fig. 9). Subsurface sediment was entrained and eroded by turbulent flow creating an elliptical subsurface tunnel that connected to the incised channel below the headwall. On August 1, 2014 a geomorphically significant runoff event collapsed and eroded the pipe system and moved the headwall 7.4 m while excavating 11.3 m^3 of sediment (Fig. 10). This single event constituted 51% of the total distance moved over the 10 year period. The 7.4 m advance stands in contrast to the overall average annual advance rate of 1.45 m from 2004 to 2014. Following the August 1, 2014 event, all subsequent observed runoff was delivered to the channel at the headwall, no lateral overfall was observed. Subsequent erosion was through headwall and sidewall slumping.

5. Discussion

This study to integrate very-high temporal resolution photography with in-situ hydrologic and topographic measurements allowed us to gain insight into both event-based erosion processes and the use of ground-based cameras for observing geomorphic change.

5.1. Erosion processes

The dominance of the single event on August 1, 2014 precludes the development of statistical relationships between precipitation and runoff, and channel head advance. However, categorized event-based erosion responses can be used to illustrate the inherent complexity of interactions between hydrologic drivers and erosion response. During monsoon season months all observed erosion was associated with runoff. However, runoff event magnitude is not well correlated with erosion event magnitude and a wide range of runoff magnitudes resulted in categorically similar erosion. This finding is consistent with previously reported attempts to relate hydrologic variables to headcut advance (DeLong et al., 2014; Montgomery, 1999), but it points to the

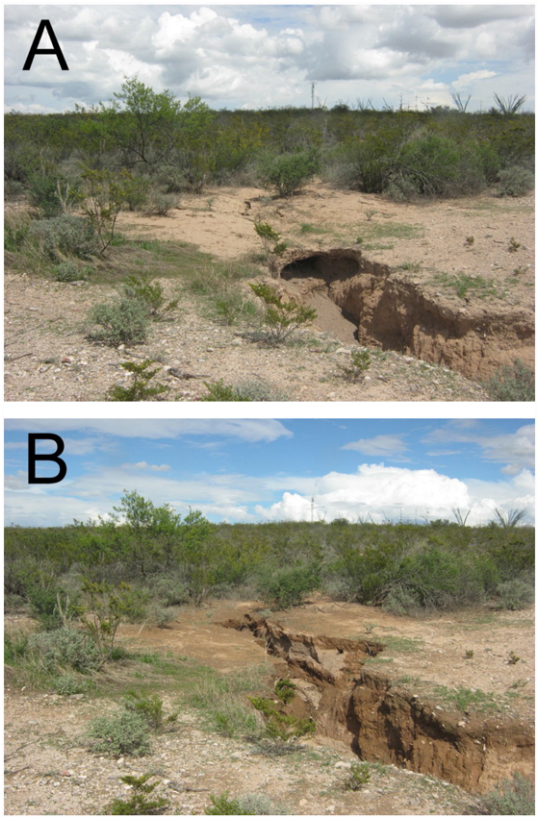

Fig. 10. Before (A) and after (B) images of the result of a 269 mm precipitation event on August 1, 2014 that generated 7 mm of runoff (peak runoff rate: 19 mm h^{-1}) and advanced the headwall 7.4 m.

need for longer-term studies to collect data sufficient to develop process-based models of headcut erosion dynamics. Mass wasting, or slumping, was observed in association with a wide range of runoff event magnitudes from 0.01 mm (peak rate 0.12 mm h^{-1}) to 15.82 mm (peak rate 39.68 mm h^{-1}). The geomorphically significant change on August 1, 2014 resulting from piping and subsurface erosion produced >50% of the total linear advance in response to a relatively small 6.51 mm flow (peak rate 19.25 mm h^{-1}). There were two runoff events during the intensive study period with magnitudes of more than twice the magnitude of the August 1, 2014 event; however, erosion during these events was limited to headwall and bank slumping.

Piping and subsurface flow erosion are important drivers of geomorphic change in many parts of the world including Asia including China (Zhu, 1997; Sidle et al., 2006), Europe (Bryan and Jones, 1997; Faulkner, 2006; Verachtert et al., 2010), and North America (Bryan and Harvey, 1985) and are an important erosion mechanism (Fox and Wilson, 2010). Early gully erosion research in Arizona (Fletcher and Carroll, 1949) and New Mexico (Leopold and Miller, 1956) described piping and subsurface flow in the southwestern US. Although regional piping in southeastern Arizona and the San Pedro Basin are well documented (Parker, 1963; Masannat, 1980), and field observations of remnant depressions in susceptible soils indicate that historically piping processes have played a role in headcut migration dynamics on WGEW (Osterkamp, pers. comm., 2014), piping has not been documented on the WGEW. This study has identified piping as an important erosion process within the WGEW. Perhaps the lack of documentation on the WGEW is because, as pointed out by Wilson (2011), unless someone is onsite at the time of collapse, the casual mechanism might be incorrectly assumed. In our case, without time-lapse photography, evaluation of before and after event photographs would not have revealed the occurrence of the piping event, and the subsequent geomorphic change would likely assumed to be the result of saturation slumping and bank failure.

Leopold and Miller (1956) observed that only a small proportion of the total flow in a gully reaches the gully by direct overpour of the vertical banks. They observed that piping tunnels and tributary gullies and rills delivered the bulk of the discharge. We observed that prior to the development of the pipe on July 25, 2014, and after the collapse and removal of the pipe system, almost all flow entered the gully by direct overpour of the banks and headwall. The direct cause of the pipe opening is not known; however, turbulent subsurface flow through a short, steep subsurface tunnel eroded sediment beneath the landscape surface.

5.2. High temporal resolution photography

Observation has a long history in geomorphology as a fundamental method for gaining insight into complex processes (Legleiter and Marston, 2013). Aerial photography has played a key role in research to quantify gully retreat rates, often in conjunction with ground measurements (Ionita, 2006; Vandekerckhove et al., 2003). Gully erosion and headcut advance have been studied across a range of time-scales form long term intervals of decades to shorter timescale at intervals of 1 to several years. The relatively long time period spanned by sequential photographs limits interpretation of linear advance to factors such as drainage basin area, but allows for assessing the influences of land-use change and management (Samani et al., 2010). The erosion response to individual runoff events is much more difficult to capture, especially in field situations where infrequent and unpredictable flash floods add logistical difficulty to collecting event based data.

Detailed images of individual runoff events and channel erosion response were captured with our time-lapse camera system. The system is readily deployable using off-the shelf components and minimal programming, but is not without limitations. Image capture was limited to daylight hours. This limitation can be overcome by incorporating infrared camera sensors or with the addition of lights (DeLong et al., 2014). We did not attempt to quantify the amounts of eroded material from the images, but by collecting stereo images with two cameras, standard photogrammetry techniques could be employed. Techniques to develop three-dimensional models using photo-reconstruction methods (Gómez-Gutiérrez et al., 2014) based on the method of structure from motion (Castillo et al., 2015) have been demonstrated for quantifying geomorphic change.

6. Conclusions

By observing the advance of an artificially induced gully head at very high temporal resolution, new insight into both event scale erosion processes and the application of time-lapse photography has been gained. Time-lapse photography showed that bank and headwall slumping, and plunge pool erosion were the most frequent erosion processes in response to flash flood runoff during the monsoon season at the study site. These processes were poorly correlated with precipitation or runoff characteristics and occurred across a range of runoff events with similar characteristics; however, soil moisture fluxes appear to be an important controlling factor. The major insight into gully headwall erosion was the occurrence of subsurface erosion. Although seepage and groundwater flow are not dominant hydrologic processes at the study site and have not been considered as geomorphic agents on the WGEW, the redirection of surface runoff to subsurface flow resulting from piping is an important and previously unreported mechanism of headcut advance on the WGEW. Time-lapse photography is an important compliment to traditional hydrologic and topographic measurement for understanding event based channel erosion processes.

Acknowledgements

The authors express their appreciation to John Smith, Michelle Cavanaugh, and the staff of the Walnut Gulch Experimental Watershed field office for field and technical assistance.

Appendix A. Supplementary data

Supplementary data to this article can be found online at http://dx.doi.org/10.1016/j.geomorph.2016.05.001.

References

Alonso, C.V., Combs, S.T., 1990. Streambank erosion due to bed degradation - a model concept. Trans. ASAE 33, 1239–1248.
Alonso, C.V., Bennett, S.J., Stein, O.R., 2002. Predicting head cut erosion and migration in concentrated flows typical of upland areas. Water Resour. Res. 38, 1303–1317.
Bryan, R.B., Harvey, L.E., 1985. Observations on the geomorphic significance of tunnel erosion in a semi-arid ephemeral drainage system. Geografiska Annaler. Series A. Phys. Geogr. 67, 257–272.
Bryan, R.B., Jones, J.A.A., 1997. The significance of soil piping processes: inventory and prospect. Geomorphology 20, 209–218.
Bull, W.B., 1997. Discontinuous ephemeral streams. Geomorphology 19, 227–276.
Castillo, C., James, M.R., Redel-Macías, M.D., Pérez, R., Gómez, J.A., 2015. SF3M software: 3-D photo-reconstruction for non-expert users and its application to a gully network. Soil 1, 583–594.
DeLong, S.B., Johnson, J.P.L., Whipple, K.X., 2014. Arroyo channel head evolution in a flash-flood-dominated discontinuous ephemeral stream system. Geol. Soc. Am. Bull. 126. http://dx.doi.org/10.1130/B31064.1.
Dietrich, W.E., Dunne, T., 1993. The channel head. In: Bevin, K., Kirkby, M.J. (Eds.), Channel Network Hydrology. John Wiley & Sons, Chichester, pp. 175–219.
Dunne, T., 1990. Hydrology, mechanics, and geomorphic implications or erosion by subsurface flow. In: Higgins, C.G., Coates, D.R. (Eds.), Groundwater Geomorphology: The Role of Subsurface Water in Earth-Surface Processes and LandformsGeological Society of America Special Paper 252. Colorado, Boulder, pp. 1–28.
Faulkner, H., 2006. Piping hazard on collapsible and dispersive soils in Europe. In: Boardman, J., Poesen, J. (Eds.), Soil Erosion in Europe. John Wiley & Sons, Chichester, pp. 537–562.
Fletcher, J.E., Carroll, P.H., 1949. Some properties of soils associated with piping in Southern Arizona. Soil Sci. Soc. Am. Proc. 13, 545–547.
Flores-Cervantes, J.H., Istanbulluoglu, E., Bras, R.L., 2006. Development of gullies on the landscape. A model of headcut retreat resulting from plunge pool erosion. J. Geophys. Res. 111. http://dx.doi.org/10.1029/2004JF000226.
Fox, G.A., Wilson, G.V., 2010. The role of subsurface flow in hillslope and stream bank erosion: a review. Soil Sci. Soc. Am. J. 74, 717–733.
Frankl, A., Poesen, J., Deckers, J., Haile, M., Nyssen, J., 2012. Gully head retreat rates in the semi-arid highlands of Northern Ethiopia. Geomorphology 173–174, 185–195.
Gómez-Gutiérrez, A., Schnabela, S., Berenguer-Sempereb, F., Lavado-Contadora, F., Rubio-Delgadoa, J., 2014. Using 3D photo-reconstruction methods to estimate gully headcut erosion. Catena 210, 91–101.
Goodrich, D.C., Schmugge, T.J., Jackson, T.J., Unkrich, C.L., Keefer, T.O., Parry, R., Bach, L.B., Amer, S.A., 1994. Runoff simulation sensitivity to remotely sensed initial soil water content. Water Resour. Res. 30, 1393–1405.
Goodrich, D.C., Keefer, T.O., Unkrich, C.L., Nichols, M.H., Osborn, H.B., Stone, J.J., Smith, J.R., 2008. Long-term precipitation database, Walnut Gulch Experimental Watershed, Arizona, United States. Water Resour. Res. 44, W05S04. http://dx.doi.org/10.1029/2006WR005782.
Goodrich, D.C., Burns, I.S., Unkrich, C.L., Semmens, D., Guertin, D.P., Hernandez, M., Yatheendradas, S., Kennedy, J.R., Levick, L., 2012. KINEROS2/AGWA: model use, calibration, and validation. Trans. ASABE 55, 1561–1574.
Graf, W.L., 1983. Variability of sediment removal in a semiarid watershed. Water Resour. Res. 19, 643–652.
Hereford, R., 1993. Entrenchment and widening of the upper San Pedro River, Arizona. Geological Society of America Special Paper 282 (46 pp.).
Ionita, I., 2006. Gully development in the Moldavian Plateau of Romania. Catena 68, 133–140.
Keefer, T.O., Moran, M.S., Paige, G.B., 2008. Long-term meteorological and soil hydrology database, Walnut Gulch Experimental Watershed, Arizona, United States. Water Resour. Res. 44, W05S07. http://dx.doi.org/10.1029/2006WR005702.
King, D., Skirvin, S., Holifield Collins, C., Moran, M.S., Biedenbender, S., Kidwell, M., Weltz, M.A., Diaz-Guiterrez, A., 2008. Assessing vegetation change temporally and spatially in southeastern Arizona. Water Resour. Res. 44, W05S15. http://dx.doi.org/10.1029/2006WR005850.
Legleiter, C.J., Marston, R.A., 2013. Introduction to the special issue: the field tradition in geomorphology. Geomorphology 200, 1–8.
Leopold, L.B., Miller, J.P., 1956. Ephemeral Streams-Hydraulic Factors and Their Relation to the Drainage Net (USGS Prof. Pap. 282-A). U.S. Government Printing Office, Washington, DC, pp. 1–37.
Masannat, Y.M., 1980. Development of piping erosion conditions in the Benson area, Arizona, USA. Q. J. Eng. Geol. 13, 53–61.
Montgomery, D.R., 1999. Erosional processes at an abrupt channel head: implications for channel entrenchment and discontinuous gully development. In: Darby, S.E., Simon, A. (Eds.), Incised River Channels: Processes, Forms, Engineering and Management. John Wiley, New York, pp. 247–276.
Nearing, M.A., Kimoto, A., Nichols, M.H., Ritchie, J.C., 2005. Spatial patterns of soil erosion and deposition in two small, semiarid watersheds. J. Geophys. Res. 110, F04020. http://dx.doi.org/10.1029/2005JF000290.
Nearing, M.A., Nichols, M.H., Stone, J.J., Renard, K.G., Simanton, J.R., 2007. Sediment yields from unit-source semi-arid watersheds at Walnut Gulch. Water Resour. Res. 43, W06426. http://dx.doi.org/10.1029/2006WR005692.
Nichols, M.H., 2006. Measured sediment yield rates from semiarid rangeland watersheds. Rangel. Ecol. Manag. 59, 55–62.
Nichols, M.H., Lane, L.J., Manetsch, C., 1993. Analysis of spatial and temporal precipitation data over a densely gaged experimental watershed. Proceeding of the American Society of Civil Engineers Irrigation and Drainage Division Conference on the Management of Irrigation and Drainage Systems, pp. 440–447.
Nichols, M.H., Nearing, M.A., Poyakov, V.O., Stone, J.J., 2013. A sediment budget for a small semiarid watershed in southeastern Arizona, USA. Geomorphology 180–181, 137–145.
Osborn, H.B., Simanton, J.R., 1986. Gully migration on a Southwest rangeland watershed. J. Range Manag. 39, 558–561.
Osborn, H.B., Simanton, J.R., 1989. Gullies and sediment yield. Rangelands 11, 51–56.
Osborn, H.B., Simanton, J.R., Renard, K.G., 1976. Use of the universal soil loss equation in the semiarid southwest. Soil Erosion: Prediction and Control, Special Pub. 21. Soil Conservation Society of America, Ankeny, Iowa, pp. 41–49.
Osterkamp, W., 2008. Geology, soils, and geomorphology of the Walnut Gulch Experimental Watershed, Tombstone, Arizona. J. Ariz. Nev. Acad. Sci. 40, 136–154.
Parker, G.G., 1963. Piping, a geomorphic agent in landform development of the drylands. Int. Assoc. Sci. Hydrol. Publ. 65, 103–113.
Poesen, J., Nachtergale, J., Vertstraeten, G., Valentin, C., 2003. Gully erosion and environmental change. Importance and research needs. Catena 50, 91–134.
Poesen, J., Torri, D.B., Vanwallenghem, T., 2011. Gully erosion: procedures to adopt when modelling soil erosion in landscapes affected by gullying. In: Morgan, R.P.C., Nearing, M.A. (Eds.), Handbook of Erosion Modelling. John Wiley, New York, pp. 361–386.
Polyakov, V., Kimoto, A., Nearing, M.A., Nichols, M.H., 2009. Tracing sediment movement on semi-arid watershed using rare earth elements. Soil Sci. Soc. Am. 73, 1559–1565.
Rengers, F.K., Tucker, G.E., 2014. Analysis and modeling of gully headcut dynamics, North American high plains. J. Geophys. Res. Earth Surf. 119. http://dx.doi.org/10.1002/2013JF002962.
Rieke-Zapp, D.H., Nichols, M.H., 2011. Headcut retreat in a semiarid watershed in the southwestern United States since 1935. Catena 87, 1–10.
Samani, A., Ahmadi, H., Mohammadi, A., Ghoddousi, J., Salajegheh, A., Boggs, G., Pishyar, R., 2010. Factors controlling gully advancement and models evaluation (Hableh Rood Basin, Iran). Water Resour. Manag. 24, 1531–1549.
Sidle, R.C., Ziegler, A.D., Negishi, J.N., Nik, A.R., Siew, R., Turkelboom, F., 2006. Erosion processes in steep terrain: truths, myths, and uncertainties related to forest management in southeast Asia. For. Ecol. Manag. 224, 199–225.
Smith, R.E., Chery, D.L., Renard, K.G., Gwinn, W.R., 1982. Supercritical flow flumes for measuring sediment-laden flow. USDA-ARS Tech. Bull. No. 1655.
Smith, R.E., Goodrich, D.C., Woolhiser, D.A., Unkrich, C.L., 1995. KINEROS - a kinematic runoff and erosion model. In: Singh, V.P. (Ed.), Computer Models of Watershed Hydrology. Water Resources Publications, pp. 697–732.
Stillman, S., Ninneman, J., Zeng, X., Franz, T., Scott, R.L., Shuttleworth, W.J., Cummins, K., 2014. Summer soil moisture spatiotemporal variability in Southeastern Arizona. J. Hydrometeorol. 15, 1473–1485.
Stone, J.J., Nichols, M.H., Goodrich, D.C., Buono, J., 2008. Long-term runoff database, Walnut Gulch Experimental Watershed, Arizona, United States. Water Resour. Res. 44, W05S05. http://dx.doi.org/10.1029/2006WR005733.
Trimble, S.W., 1999. Decreased rates of alluvial sediment storage in the Coon Creek Basin, Wisconsin, 1975–93. Science 285, 1244–1246.
USDA, 2003. Soil Survey of Cochise County, Arizona, Douglas-Tombstone Part. USDA-ARS, Washington, DC.
Vandekerckhove, L., Poesen, J., Govers, G., 2003. Medium-term gully headcut retreat rates in Southeast Spain determined from aerial photographs and ground measurements. Catena 50, 329–352.
Verachtert, E., Van Den Eeckhaut, M., Poesen, J., Deckers, J., 2010. Factors controlling the spatial distribution of soil piping erosion on loess-derived soils: a case study from central Belgium. Geomorphology 118, 339–348.
Weltz, M.A., Ritchie, J.C., Fox, H.D., 1994. Comparison of laser and field measurements of vegetation heights and canopy cover. Water Resour. Res. 30, 1311–1319.
Wilson, G., 2011. Understanding soil-pipe flow and its role in ephemeral gully erosion. Hydrol. Process. 25, 2354–2364.
Zhang, Y., Nearing, M.A., Wei, H., 2011. Effects of antecedent soil moisture on runoff modeling in small semiarid watersheds of southeastern Arizona. Hydrol. Earth Syst. Sci. 15, 3171–3179.
Zhu, T.X., 1997. Deep-seated, complex tunnel systems-a hydrological study in a semi-arid catchment, Loess Plateau, China. Geomorphology 20, 255–267.